Supplementary S1. Other figures of Contact angle change

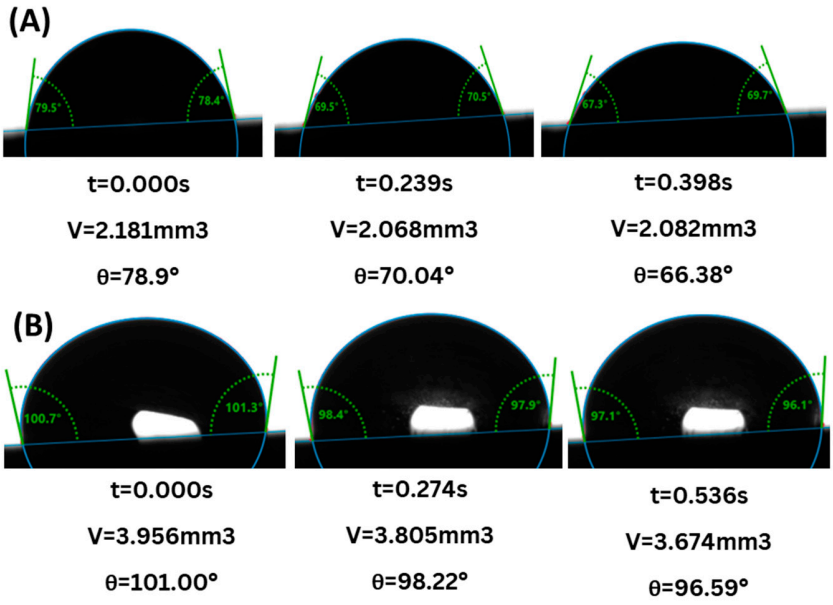

Figure S1. Sequential digital images of the sessile water drop on the $scCO_2$-saturated sandstone substrate sample 1S (A) Pretest CA (B) Post-test CA after 24hrs of CCI of $scCO_2$.

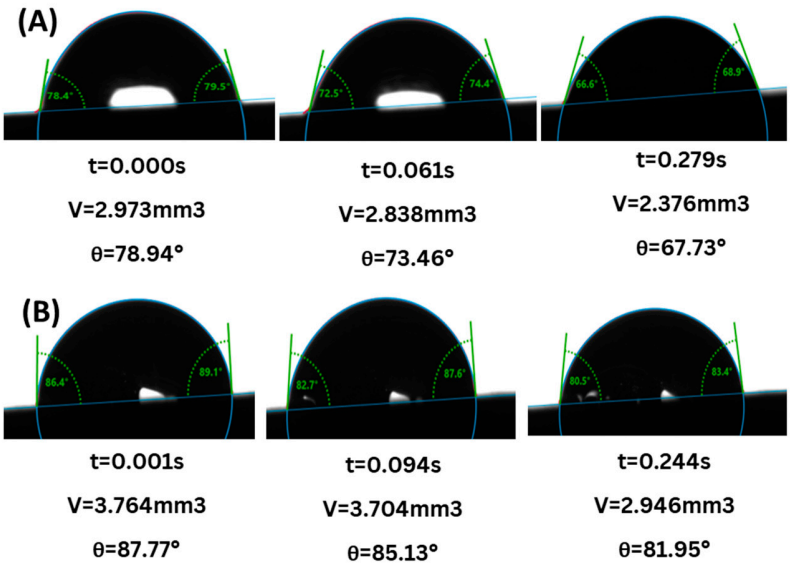

Figure S2. Sequential digital images of the sessile water drop on the $scCO_2$-saturated sandstone substrate sample 2S (A) Pretest CA (B) Post-test CA after 24hrs of WAG of $scCO_2$ and water.

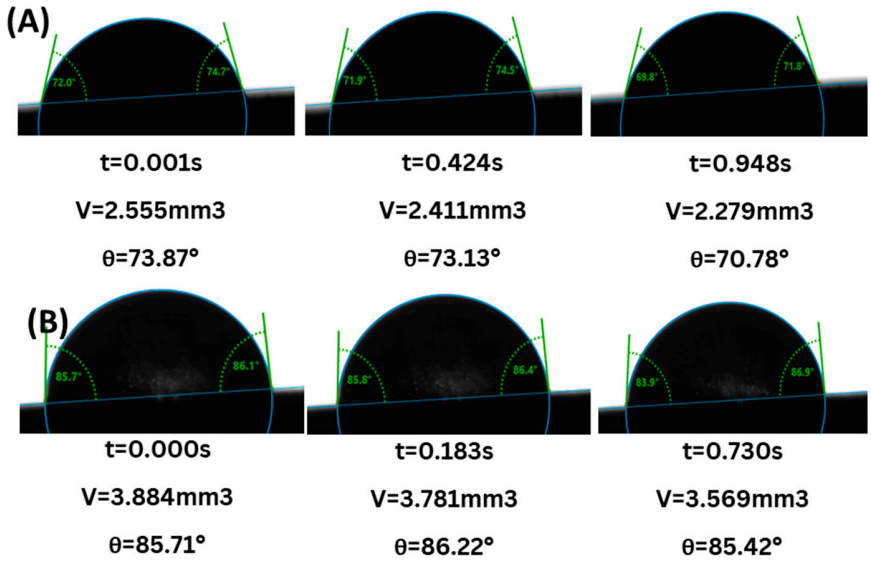

Figure S3. Sequential digital images of the sessile water drop on the $scCO_2$-saturated sandstone substrate sample 3S (A) Pretest CA (B) Post-test CA after 24hrs of SAI of $scCO_2$ and water.

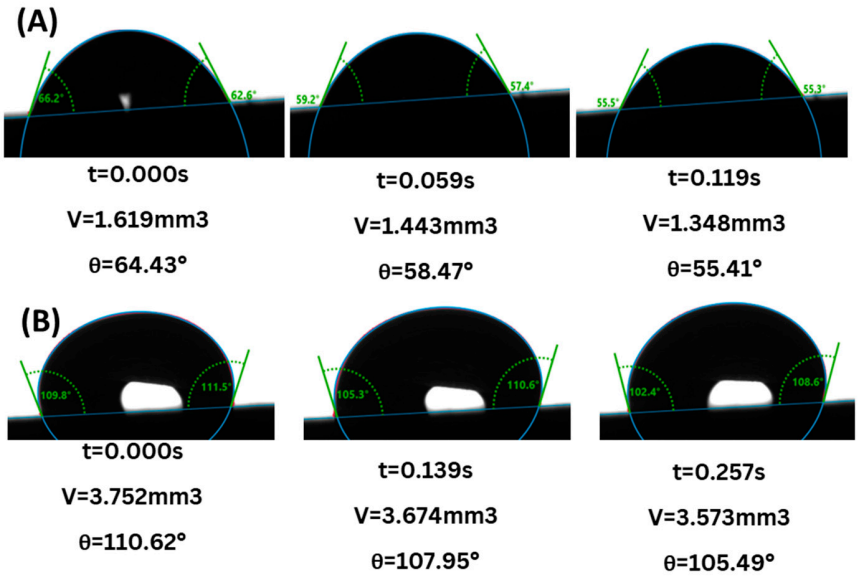

Figure S4. Sequential digital images of the sessile water drop on the $scCO_2$-saturated sandstone substrate sample 4S (A) Pretest CA (B) Post-test CA after 72hrs of CCI of $scCO_2$.

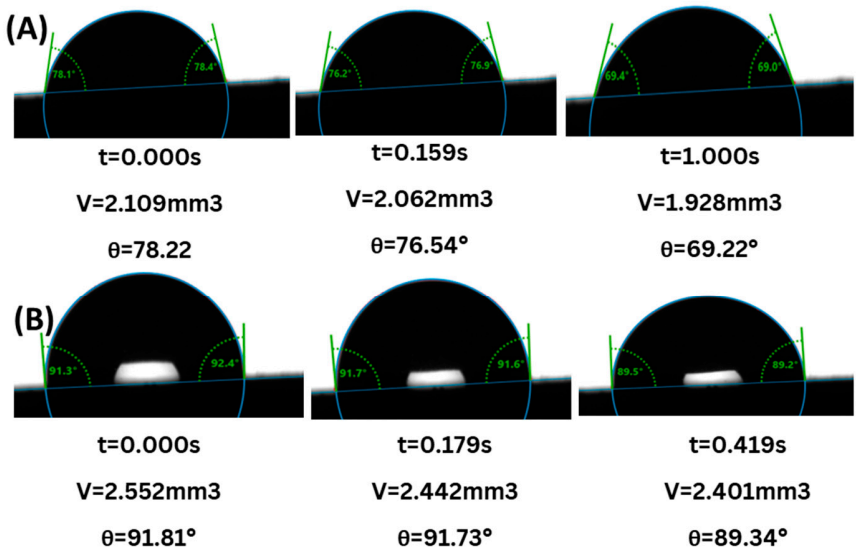

Figure S5. Sequential digital images of the sessile water drop on the $scCO_2$-saturated sandstone substrate sample 5S (A) Pretest CA (B) Post-test CA after 72hrs of WAG of $scCO_2$ and water.

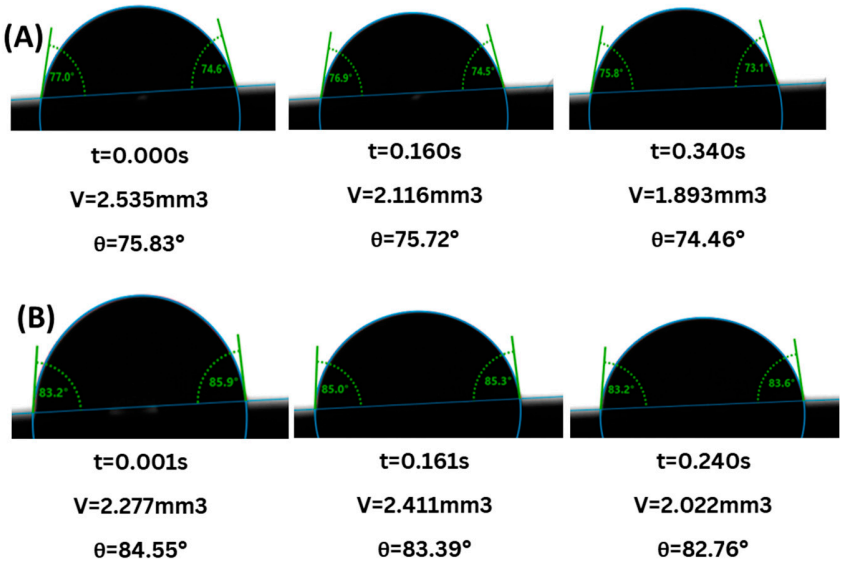

Figure S6. Sequential digital images of the sessile water drop on the $scCO_2$-saturated sandstone substrate sample 6S (A) Pretest CA (B) Post-test CA after 72hrs of SAI of $scCO_2$ and water.

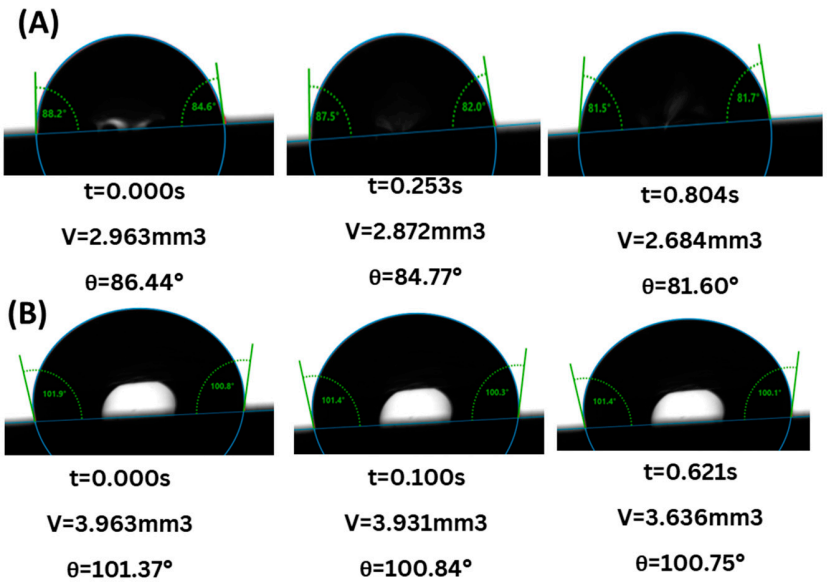

Figure S7. Sequential digital images of the sessile water drop on the $scCO_2$-saturated sandstone substrate sample 1L (A) Pretest CA (B) Post-test CA after 24hrs of CCI of $scCO_2$.

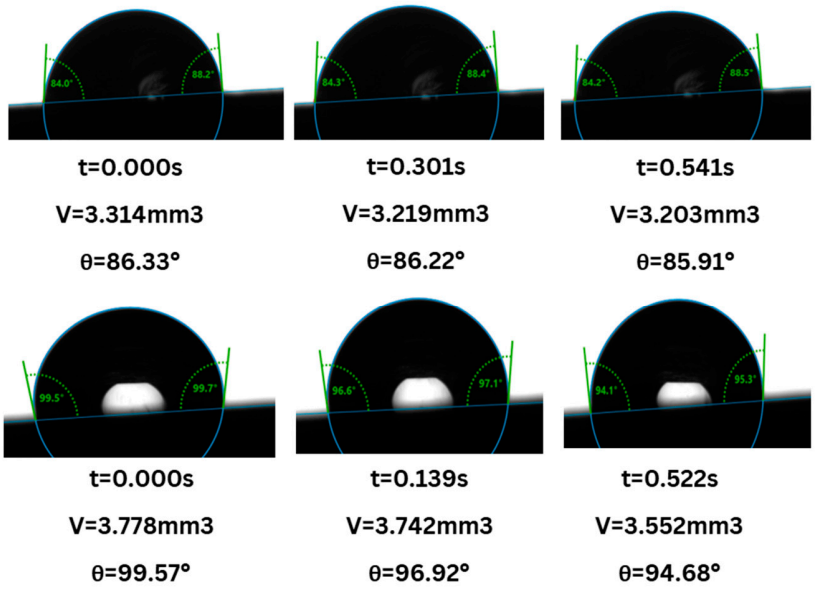

Figure S8. Sequential digital images of the sessile water drop on the $scCO_2$-saturated sandstone substrate sample 2L (A) Pretest CA (B) Post-test CA after 24hrs of WAG of $scCO_2$ and water.

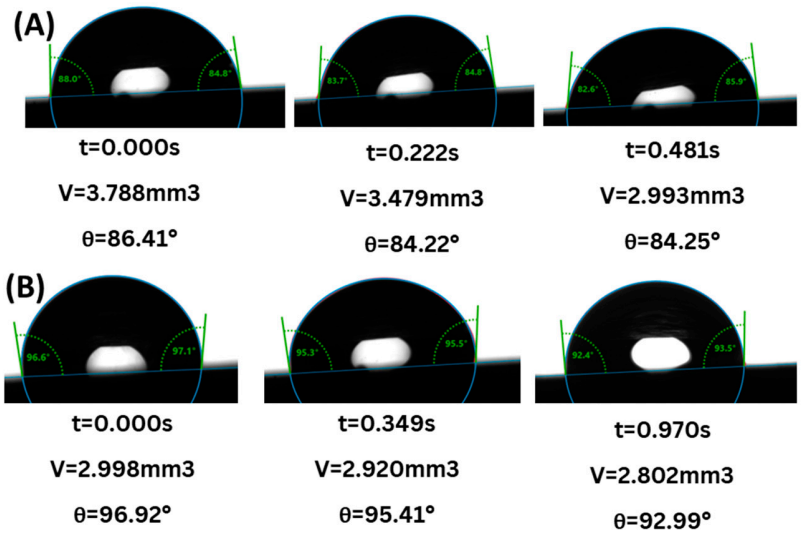

Figure S9. Sequential digital images of the sessile water drop on the $scCO_2$-saturated sandstone substrate sample 3L (A) Pretest CA (B) Post-test CA after 24hrs of SAI of $scCO_2$ and water.

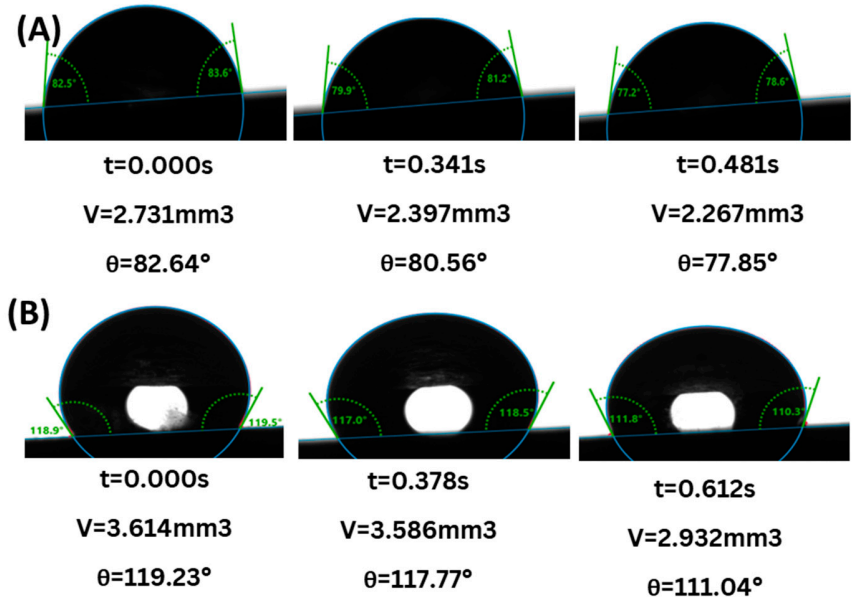

Figure S10. Sequential digital images of the sessile water drop on the $scCO_2$-saturated sandstone substrate sample 4L (A) Pretest CA (B) Post-test CA after 72hrs of CCI of $scCO_2$.

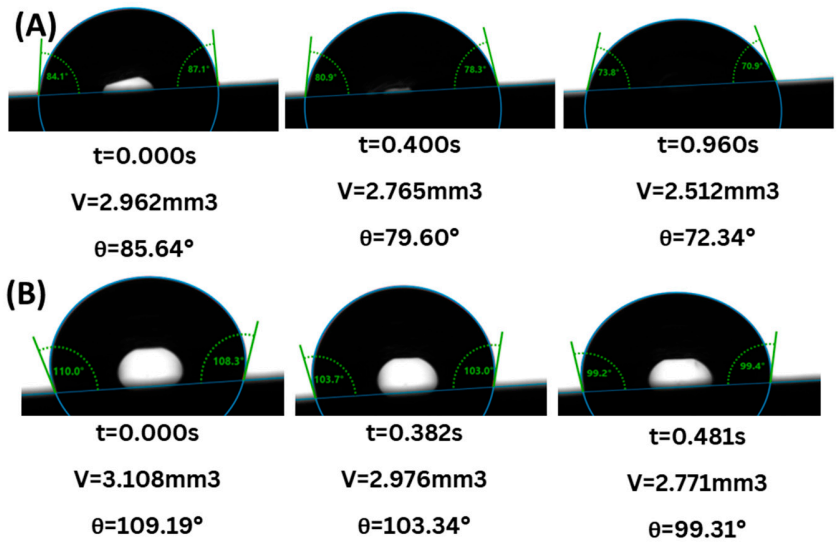

Figure S11. Sequential digital images of the sessile water drop on the $scCO_2$-saturated sandstone substrate sample 5L (A) Pretest CA (B) Post-test CA after 72hrs of WAG of $scCO_2$ and water.

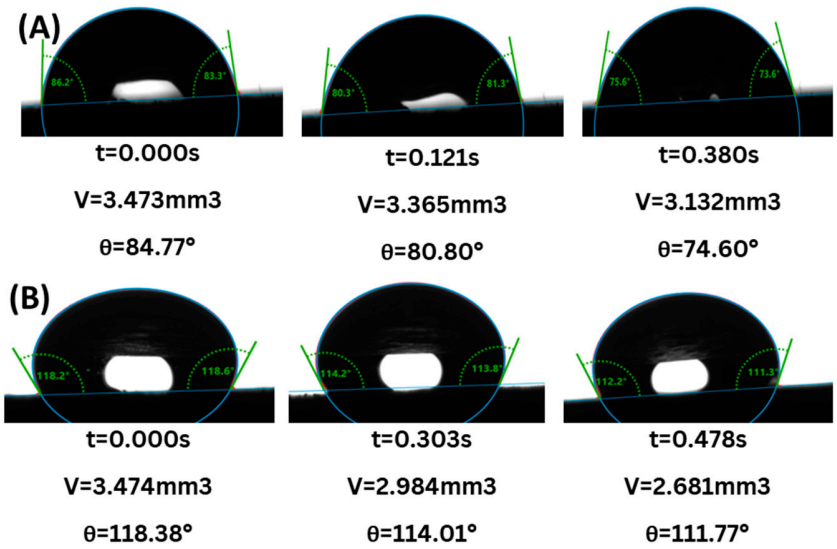

Figure S12. Sequential digital images of the sessile water drop on the $scCO_2$-saturated sandstone substrate sample 6L (A) Pretest CA (B) Post-test CA after 72hrs of SAI of $scCO_2$ and water.

Supplementary S2: Contact angle and wettability

Table S1. Effect of Pressure on Contact Angle and wettability

Effect of Pressure on CA and Wettability						
Type of Study	**Methods**	**Experimental /reservoir condition**	**Type of interaction**	**Causes and Effects studied**	**Impact on Wettability**	**Reference**
Experimental	novel high-pressure	Pressure range- 204bar Temperatures at 38-55 °C	CO2-Water–solid Hydrophilic surface	CA increased significantly as the system pressure increased from atmospheric pressure to 204 bar and remained constant afterward.	Wettability changed from strongly water-wet to less water-wet	[78]
	Captive-drop technique	Pressure range-1 MPa - 11MPa. Temperature - 308k, Salt concentration- 0.2M	CO2-Brine-mineral system Mineral type - Quartz and Muscovite Mica	CA increases from approximately 22° to 38° with increasing pressure for quartz, and the effect is higher in mica, i.e., quartz and mica become less water-wet in the presence of dense CO2.	Wettability changed from water-wet to less water-wet	[35]
	Sessile drop	Pressure range-14.7 MPa -10MPa. Temperature – 313-353k	CO2-Oil-Brine-rock system Mineral type -Calcium carbonate crystals, limestone, sandstone, and dolomite	CA decreases with pressure. The contact angle is 95.98° at the beginning. Gradually, it is reduced and reaches its constant value of 89.45° at equilibrium.	Wettability changed from a strongly oil-wet situation to a weakly oil-wet situation.	[79]
	Dynamic sessile brine drops and USBM/Amott wettability	Pressure range-0.34 - 20MPa. Temperature – 323.2 K Reservoir brine is 1.045 g/cm3 at 15 °C	CO2-Oil-Brine-rock system Mineral type-Calcite, limestone, sandstone, dolomite	CA is diminished in the presence of CO2 at rising pressure. After nearly 90 minutes of decreasing CA, a constant value is established at 20MPa.	Wettability changed from oil-wet situation to strongly water-wet for calcite and sandstone, while limestone and dolomite are intermediate water-wet	[25]
	Captive bubble technique	Pressure range-0.8 - 14MPa. Temperature – 35-140°C Brine density-140 g/L NaCl	CO2-water-mineral Mineral type -Carbonate-rich caprock	CA remains constant from 0.8MPa to 14MPa through a series of CA measurements on substrates.	Wettability remains strongly water-wet	[80]
	Sessile droplet method	Pressure range-0.1 - 20MPa. Temperature – 298K Solution molarity of 0.2 M	CO2-brine-Mineral and CO2-Oil-Brine-Mineral Mineral type - Amorphous silica, Calcite substrate	For the CO2-brine-Mineral system, CA remains constant at 40° while the CA on the oil-wet silica increases slightly (from 85° to 90°) when CO2 pressure increases from 0.1 MPa to 6.43 MPa at 298K	For the CO2-brine-Mineral system, there was no change in wettability, while in the case of the CO2-Oil-Brine-Mineral system, the substrate turns from slightly hydrophilic to hydrophobic upon pressurization	[81]
	Sessile drop CA method	Pressure range-1.4-20.7MPa Temperature – 294.14-323.15K	CO2-water-Mineral Mineral type – Quartz and Calcite	CA increased slightly with pressure from 200-800psig; however, the CO2 phase became liquid or supercritical. There is a dip in CA when pressure increases from 800-3000 psi for both quartz and calcite.	Wettability remains strongly water-wet	[36]

	Captive bubble technique	Pressure increases from 5.8Mpa to 13MPa, Temperatures at 313.15K and salinity at 35000ppm	CO2-brine-Mineral Mineral type –Quartz, Orthoclase, Labradorite, Calcite and Biotite	For quartz and biotite, CA decreases with an increase in pressure. For mica and calcite, CA increases as pressure increases or vice versa.	The wettability changes from Strongly water-wet to intermediate water-wet condition for quartz and biotite. At the same time, mica and calcite became more water-wet.	[37]
	Captive needles drop method	Pressure range-0.5-11.4MPa Temperature– 9.35 and 120°C Brine density-4, 40, and 350g NACl/l for low, moderate, and high-salinity brine.	CO2-brine-rock system Mineral type- Mica, Quartz, and calcite-carbonate-rich rock	CA increases with pressure for all minerals except for quartz, which remains constant.	All the mineral surfaces became less water-wet except for the quartz system, which remained constant-strongly water-wet	[82]
	Sessile drop	Pressure range-0.1-25MPa. Temperature– 45°C Brine density-0-5M NaCl	CO2−brine-Silica systems	Water CAs on silica increased within a pressure range of 7-10Mpa and remained constant above 10MPa.	Wettability changed from strongly water-wet for quartz to less water-wet for quartz.	[83]
	Captive bubble-pendent	Pressure range-0.1-16MPa. Temperature – 318K Brine density-5000, 20000, and 35000mg/L for low, moderate, and high salinity brine	CO2-brine-Oil-wet substrate system, Mineral-quartz with minor feldspar and clay (Aging time 22 months at 333K)	CA increases as pressure increases and remains constant beyond 10MPa	Carbon dioxide becomes the wetting phase at pressures higher than 10.0 MPa.	[28]
	Captive bubble using needles drop method	Pressure range-0-30MPa. Temperature – 36°C Brine density 0.8M NaCl Exposure days-50days	CO2-brine-rock system Mineral-quartz, calcite, and feldspar	No significant change in CA change in pressure	Quartz, feldspar, and calcite remained strongly water-wet	[84]
	Captive bubble- ADSA-NA[1]	Pressures 14-27MPa, Temperatures-50–100°C Brine salinities-0.2–5 M	CO2-brine-quartz systems.	Water-receding CAs were only slightly affected by changes in P and T. Water-advancing CA slightly increased with increasing the pressure and mildly decreased with increasing the temperature, creating an overall canceling effect.	Wettability remains strongly water-wet	[26]
	Sessile drop	Pressures-3.0 -9.0 MPa Temperatures-27-408°C Brine salinities- 0.102 and 1.0 mol/L	CO2-NaCl-quartz	CAs increased with pressure	Wettability changed from strongly water-wet to less water-wet	[27]
	Sessile drop-tilting plate	Pressure range- 0.1MPa-20MPa, Temperatures at 296-343K	CO2-water-quartz system	Water CA increased with pressure,	Wettability changed from strongly water-wet to less water-wet.	[18].

[1] ADSA-NA-Axisymmetric Drop Shape Analysis with no-Apex

		salinity-0.35%wt NaCl, CaCl2, MgCl2 at 35000ppm surface roughness 56-1300 nm				
	Sessile drop	Pressure range- 0.1MPa to 20MPa, Temperatures at 308-343K, and salinity-0-30% weight NaCl. surface roughness ~ 12nm	CO2-brine-mica system	The results indicate that both advancing and receding contact angles increase with pressure.	At 20 MPa and 308K, the advancing angle is measured to be ~110o, indicating CO2-wetting.	[22]
	Sessile drop	Pressure range- 0.1-20MPa Temperatures - 296-343K	CO2-brine-mineral system	CA continuously increased with increasing pressure from 35° to 56°	Wettability changed from strongly water-wet to less water-wet.	[19]
	Captive bubble	Pressure range- 0.7-24MPa Temperatures - 38°C	CO2-brine-Oil-rock system Mineral type-Quartz, mica, and calcite	The CAs. Decrease from 76°, 89°, and 144° to 61°, 63°, and 97° for quartz, mica, and calcite, respectively, with an increase in pressure.	Wettability changed from mixed-wet or oil-wet to water-wet	[85]
	Captive bubble	Pressure range- 2-25MPa Temperatures -40°C and salinity-5.19M	CO2-brine-mineral interface Mineral Type-Sandstone and limestone-Quartz, Illite, Microcline	The CAs. increase when pressure is increased from 2 to 7.38 MPa at 40°C and remain constant above 7.38MPa for all minerals.	Wettability changed from strongly water-wet to less water-wet	[23]
	Sessile drop	Pressure range-3–15 MPa, Temperature -50 °C, 100 °C Brine density-1.98 mol/Kg NaCl	CO2– deionized sandstone. CO2– brine-sandstone	The CAs. increase when pressure is increased.	Wettability changed from strongly water-wet to less water-wet	[20]
	Sessile drop	Pressure range-3–15 MPa, Temperature -50 °C, 100 °C Brine density-1.98 mol/Kg NaCl	CO2– brine-rock (Quartz and microcline)	The CAs. increase when pressure is increased	Three rock samples became less water-wet when the CO2 phase state changed from subcritical to supercritical.	[24]
Simulation-molecular dynamics	EPM2-TIP4/2005	Pressure range-0-20MPa. Temperature-300-350k salinity - 1M to 4M	CO2-brine-rock (Quartz-water-CO2)	The CA increased from 0 to 80° but no significant increase after the saturation pressure of 6.7MPa	Quartz becomes less water-wet.	[86]
		Pressure range-0-10MPa. Temperature-296-348K Salinity - 1.2-4.8mol/l	CO2-water-hydrophilic Silica system (Hydrophilic silica)	No Change in CA	CA calculations showed that wettability is independent of pressure change	[87]
	Combination of TraPPE/TIP4P 2005 and EPM2/SPC	Pressure range- 3.4-12MPa, Temperatures - 300-333K.	CO2-water-quartz systems (α-quartz surface)	CA slightly decreased by 1–4 deg in the presence of H2CO3 across the pressure range investigated. This may be attributed to an error in measurement.	Wettability remains unchanged	[15]
	The half-cylindrical	Pressure range- 2.8-32.6MPa, Temperatures - 318-383K.	CO2-brine-silica (Silica, crystalline silica, and amorphous silica)	For crystalline and amorphous silica, water CA first increases at P=8-12Mpa, then decreases and finally keeps constant	Wettability changed from water-wet to less water-wet.	[88]

	water droplets method was			with pressure; however, the amorphous contact angle increase is larger than crystalline		
	Molecular dynamic	Pressure range- 0-200MPa Temperatures at 323-443K	Alkane-water-silica and alkane+CO2+water-silica systems	This contact angle decreases with pressure; the higher the temperature, the more pronounced the pressure effect. The contact angles of the CO2+water+silica system were in reasonable agreement with experimental data. The contact angle increased with increasing pressure.	Wettability changes from more water-wet to less water-wet surface	[89]

Table S2. Effect of Temperature on Contact Angle and wettability

Effect of Temperature on CA and Wettability						
Type of Study	**Methods**	**Experimental /reservoir condition**	**Type of interaction**	**Causes and Effects studied**	**Impact on Wettability**	**Reference**
Experimental	Captive bubble technique	Pressure range-0.8 -14MPa. Temperature – 35-140°C Brine density-140 g/L NaCl	CO2-water-mineral systems Mineral type - Carbonate-rich caprock	CA remains constant with an increase in temperature. Interestingly, the contact angle hysteresis, i.e., the difference between the advancing and receding angles, is observed to be almost zero in all measurements.	Wettability remains strongly water-wet	[80]
	Sessile drop CA method -Set	Pressure range-200-3000psig. Temperature – 77-122°F	CO2-water-Mineral Mineral type – Quartz and Calcite	For Quartz, CA decreases from about 45 to 20° for quartz and calcite	Wettability remains strongly water-wet	[36]
	Wilhelmy plate	Pressure range- 14.7psia Temperature – 323-343K	CO2-brine-rock Mineral type – Quartz and Calcite	The contact angle results show with the increasing CO2 partial pressure, the contact angle of water on the reservoir rock surface increases at 323K and decreases at 343K.	Wettability changed from strongly water-wet to less water-wet	[90]
	Captive bubble	Pressure range-0-30MPa. Temperature – 36°C Brine density 0.8M NaCl Exposure days-50days	CO2-brine-rock system Mineral-quartz, calcite, and feldspar	Slight changes in CA with temperature increase.	Wettability remains strongly water-wet	[84]
	Combination of TraPPE/TIP4P2005 and EPM2/SPC	Pressure range- 3.4-12MPa, Temperatures -300-333K.	CO2-water-quartz systems (α-quartz surface)	CA increased with increasing temperature	Wettability changed from strongly water-wet to less water-wet	[15]
	Sessile drop-tilting plate	Pressure range-0.1MPa-20MPa, Temperatures at 296-343K and salinity-0.35%wt NaCl, CaCl2, MgCl2 at 35000ppm Surface roughness-56-1300nm	CO2-water-quartz system	Water CA increased with temperature,	Wettability changed from strongly water-wet to less water-wet	[18]

	Sessile drop	Pressure range- 0.1MPa to 20MPa, Temperatures at 308-343K, and salinity-0-30% weight NaCl. surface roughness ~ 12nm	CO2-brine-mica system	The results indicate that both advancing and receding contact angles decrease with temperature.	Wettability changed from strongly water-wet to less water-wet	[22]
	Sessile drop	Pressure range- 0.1-20MPa Temperatures -296-343K	CO2-brine-mineral system	CA increased with increasing temperature	Wettability changed from strongly water-wet to less water-wet	[19]
	Sessile drop	Pressure range-3–15 MPa, Temperature -50 °C, 100 °C Brine density-1.98 mol/Kg NaCl	CO2– deionized sandstone. CO2– brine-sandstone	The results showed that the contact angle increases with an increase in temperature.	Wettability changed from strongly water-wet to less water-wet	[20]
Simulation-molecular dynamics	half-cylindrical water droplets method	Pressure range- 2.8-32.6MPa, Temperatures -318-383K	CO2-brine-silica (Silica, crystalline silica, and amorphous silica)	As temperature increases, water CA decreases.	Wettability changed from strongly water-wet to less water-wet	[88]
	Molecular dynamic	Pressure range- 0-200MPa Temperatures at 323-443K	Alkane-water-silica and alkane+CO2+water-silica systems	The contact angle decreased with the increasing temperature of this system.	The wettability changes from less water-wet to more water-wet surface	[89]

Table S3. Effect of Salinity on Contact Angle and wettability

Effect of Salinity on CA and Wettability						
Type of Study	**Methods**	**Experimental /reservoir condition**	**Type of interaction**	**Causes and Effects studied**	**Impact on Wettability**	**Reference**
Experimental	Surface force Apparatus	Salinity-1mM-1M PH-4.6-10.5	Brine-Oil mineral system mineral type-Quartz and Muscovite Mica	Intermediate wet at low salinity and water-wet at high salt concentration	Wettability changed from Intermediate-wet at low salinity to water-wet at high salinity	[91]
	Captive-drop technique	Salinity- 0.01, 0.1, 0.2, 0.5 and 1.0M	CO2-brine-mineral system mineral type-Quartz and Muscovite Mica	An increase in CA by 25° in mica. The impact of brine salinity on wettability seems to be limited in the case of quartz. In contrast, for Mica, CA increases with salinity.	Wettability changed from water-wet to less water-wet for mica, and no impact on quartz.	[30,35]
	Sessile droplet	Pressure range-0.1 -20MPa. Temperature – 298K Solution molarity of 0.2 M	CO2-brine-Mineral Mineral type - Amorphous silica, Calcite substrate	CA increases by 20° when 200gNacl/kg is added to deionized water.	Wettability changed from water-wet to less water-wet.	[81]
	Captive needles drop method	Pressure range-0.5-11.4MPa Temperature– 9.35 and 120°C Brine Concentration-4, 40 and 350g NaCl/l, for low, moderate and high-salinity' brine	CO2-brine-rock system Mineral type- Mica, Quartz, and calcite-carbonate-rich rock	As salinity increases, CA increases, making the surfaces less water-wet.	Wettability changed from water-wet to less water-wet.	[82]

	Micromodel and image analysis	Pressure- 8.5MPa Temperature– 45°C Brine density-01-5.0M NaCl concentration	scCO2-brine–silica system	CA increases within single pores. The brine CAs increased from initial values near 0° up to 80° with larger increases under higher ionic strength conditions.	Wettability changed from Strongly water-wet to weakly water-wet.	[38]
	Sessile drop	Pressure range-0.1-25MPa. Temperature– 45°C Brine density-0-5M NaCl	CO2–brine-Silica systems	CA increased with ionic strength nearly linearly	Wettability changed from Strongly water-wet to weakly water-wet.	[83]
	Captive bubble-pendent	Pressure range-0.1-16MPa. Temperature – 318K Brine density-5000, 20000, and 35000mg/L for low, moderate, and high-salinity brine	CO2-brine-Water-wet substrate system, Mineral quartz with minor feldspar and clay	At a constant pressure, the CA decreases with increasing brine salinity.	Wettability changed from less water-wet to more water-wet.	[28]
	Captive bubble	Pressure range-0-30MPa. Temperature – 36°C Brine density 0.8M NaCl Exposure days-50days	CO2-brine-rock system Mineral-quartz, calcite, and feldspar	CA decreases with salinity increase.	Wettability changed from Strongly water-wet to weakly water-wet	[84]
	Captive bubble-ADSA-NA	Pressures- 14-27MPa, Temperatures-50–100°C Brine salinities-0.2–5 M	CO2/brine/quartz systems.	The increase in brine salinity caused a considerable increase in advancing CA and a slight increase in water-receding CA.	Wettability changed from Strongly water-wet to weakly water-wet	[26]
	Sessile drop	Pressure range- 0.1MPa to 20MPa, Temperatures at 308-343K, and salinity-0-30% weight NaCl. surface roughness ~ 12nm	CO2-brine-mica system	The results indicate that both advancing and receding contact angles increase with salinity.	Wettability changed from Strongly water-wet to weakly water-wet	[22]
	Sessile drop	Pressures-3.0 to 9.0 MPa 14-27MPa, Temperatures-27 to 408°C Brine salinities- 0.102 and 1.0 mol/L concentrations	CO2-NaCl-quartz	CAs increased with NaCl concentrations increased pronounced	Wettability changed from water-wet to weakly water-wet	[27]
	Sessile drop-tilting plate	Pressure range- 0.1MPa to 20MPa, Temperatures at 296-343K and salinity-0.35%wt NaCl, CaCl2, MgCl2 at 35000ppm surface roughness 56 to 1300 nm	CO2-water-quartz system	Water CA increased with brine salinity	Wettability changed from strongly water-wet to less water-wet	[18].
	Sessile drop	Pressure range-3–15 MPa, Temperature -50 °C, 100 °C Brine density-1.98 mol/Kg NaCl	CO2– deionized sandstone. CO2– brine-sandstone	The results showed that the contact angle decreases with an increase in salinity.	Wettability changed from water-wet to more water-wet	[20]

Simulation-molecular dynamics	EPM2-TIP4/2005	Pressure range-0-20MPa. Temperature-300-350k salinity - 1M to 4M	CO2-brine-rock (Quartz-water-CO2)	Neither increase nor decrease in CA	Wettability remained strongly water-wet	[86]
	EPM2 - TIP4P-2005	Pressure - 4MPa. Temperature-300k salinity -1M to 4M	CO2-water-quartz contact	Salinity has a minor effect on the CA-divalent salts such as CaCl2	No change in wettability	[92]
	The half-cylindrical water droplets method was	Pressure range- 2.8-32.6MPa, Temperatures -318-383K	CO2-brine-silica (Silica, crystalline silica and amorphous silica)	As brine concentration increases, water CA increases.	Wettability changed from strongly water-wet to less water-wet	[88]
	semi-flexible EPM2 model	Pressure-20MPa, Temperatures -318.15K Four types of brine- NaCl, KCl, CaCl2 and MgCl2	CO2-brine-mineral systems	For MgCl2 and NaCl solutions, CA increases with salinity. For CaCl2 and KCl solutions, CA first increases and then keeps constant with salinity.	Wettability changed from strongly water-wet to less water-wet	[93]

Table S4. Effect of other properties on Contact Angle and wettability

Effect of Other Properties on CA and Wettability						
Type of Study	**Methods**	**Experimental /reservoir condition**	**Type of interaction**	**Causes and Effects studied**	**Impact on Wettability**	**Reference**
Experimental	Sessile drop CA method	Increase in no of the CO2 exposure cycle	CO2-water-Mineral Mineral type – Quartz and Calcite	CA increased with the CO2 exposure cycle from 25-30° in the first cycle to 65-70° in the second cycle.	Wettability changed from strongly water-wet to intermediate water-wet.	[36]
	Captive bubble technique	Pressure range- 5.8MPa to 13MPa, Temperatures at 313.15K and salinity at 35000ppm	CO2-brine-Mineral Mineral type –Quartz, Orthoclase, Labradorite, Calcite and Biotite	CA decreased with increase in CO2 exposure from 38-40° to 27-38°	Wettability changed from less water-wet to strongly water-wet conditions for all the gas and supercritical measurements of CO2	[37]
	Captive bubble	pH 3.1-5.9	CO2–brine–mineral system Mineral type -Quartz, calcite, microcline, kaolinite, illite, and phlogopite	CA decreases with PH increase for quartz and microcline and increases for calcite; however, it remains constant for kaolinite, illite, and phlogopite.	Quartz and microcline become more water-wet, while calcite becomes less water-wet. No change in wettability for kaolinite, illite, and phlogopite	[76]
	Captive bubble	Pressure range- 7MPa to 13MPa, Temperatures-70°C	Carbonated brine-oil-mineral system Mineral type- Carbonate	CA decreased from 101º initially to reach a stable value of about 83.9º after 44 minutes of exposure to the carbonated brine, and a second result shows that it decreased to 69.3 and remained after 34 minutes of exposure.	Rock wettability is altered from oil-wet to intermediate-wet when the oil/rock system is exposed to dissolved CO2	[94]

	Captive bubble	Pressure range- 0.2-15MPa, Temperatures at 318K.	CO2-water-quartz system	Water CAs increased with surface roughness increase	The wettability of quartz becomes less water-wet when the surface roughness is high.	[31].
	Sessile drop-tilting plate	Pressure range- 0.1MPa to 20MPa, Temperatures at 296-343K and salinity-0.35%wt NaCl, CaCl2, MgCl2 at 35000ppm surface roughness 56 to 1300 nm	CO2-water-quartz system	Water CAs decreased with surface roughness increase	The wettability of quartz becomes more strongly water-wet when the surface roughness is high.	[18].
	Micro-CT	Pressure range- 8MPa, Temperatures at 40 °C and salinity-6 wt% KCI brine	CO2-brine-quartz system	The average CA increases when gaseous CO2 (gCO2) turns into supercritical CO2 (scCO2).	Wettability changes from more water-wet to less water-wet surface	[17]
	Sessile drop	Pressure range- 13.8MPa, Temperatures at 20 °C	CO2-brine-mineral system Mineral type-quartz, feldspar.	Contact angle increases with increasing surface roughness	The wettability of quartz becomes less water-wet when the surface is high.	[4]
	Sessile drop-tilted plate technique	Pressure range- 25MPa, Temperatures at 50 °C	CO2-brine-acid -Quartz Acid-hexanoic acid, lauric acid, stearic acid and lignoceric acid	The effect of the trace of organic acid on wettability	The quartz surface turned significantly less water-wet with increasing organic acid concentrations, even at trace concentrations. Importantly, we identified a threshold concentration at ˜10^{-6} M organic acid, above which quartz wetting behavior shifts from strongly water-wet to an intermediate-wet state.	[95]
	Captive bubble	Pressure range = 5-15MPa Temperatures = 25-60°C	CO2-Oil- Water-mineral system Mineral type-Sandstone, limestone, and calcite	The presence of CO2 in LSW causes a decrease in pH and further enhances water-wettability, and seawater-CO2 systems cause salt precipitation and mineralogical changes in carbonate and sandstone rock.	The wettability changes from less water-wet to more water-wet surface.	[96]
	Nuclear Magnetic Resonance (NMR)	Pressure range = 1.01325MPa Temperatures = 298.15K Acidity-0.01 M NaOH solution to attain a pH of 8 Salinity- 1–100 mg/L in 0.3 mol. dm− 3 NaCl	NaCl brine-clean sandstone systems	zeta potential/ streaming potential was measured	The presence of organic acid changes wettability towards CO2 wet in pores, resulting in lower residual water saturation in aged cores compared to pristine cores.	[97,98]
Simulation-molecular dynamics	Standard SPC/E model	Increase CO2 fluid density while salinity and temperature remain constant	CO2-water-solid interfaces (Hydrophilic and hydrophobic surfaces)	CA of hydrophilic surface increases as CO2 density increases	Wettability changes from more water-wet to less water-wet surface	[99]
	Combination of TraPPE/TIP4P2005 and EPM2/SPC	Pressure range- 3.4-12MPa, Temperatures -300-333K.	CO2-water-quartz systems (α-quartz surface)	CA increases at a constant temperature of 308K, indicating less water-wettability due to increased CO2 density.	Wettability changes from more water-wet to less water-wet surface	[15]

	Molecular dynamic	Pressure range- 0-200MPa Temperatures at 323-443K	Alkane-water-silica and Alkane-CO2-water-silica systems	Overall, the contact angle is higher for lower and cyclic alkanes. Still, branching has no noticeable effect on the contact angle.	Lower n-alkanes are less water-wet than higher n-alkanes.	[89]

References

1. Dickson, J.L.; Gupta, G.; Horozov, T.S.; Binks, B.P.; Johnston, K.P. Wetting Phenomena at the CO_2/Water/Glass Interface. *Langmuir* **2006**, *22*, 2161–2170. https://doi.org/10.1021/la0527238.
2. Yang, D.; Gu, Y.; Tontiwachwuthikul, P. Wettability Determination of the Reservoir Brine−Reservoir Rock System with Dissolution of CO_2 at High Pressures and Elevated Temperatures. *Energy Fuels* **2007**, *22*, 504–509. https://doi.org/10.1021/ef700383x.
3. Tonnet, N.; Broseta, D.F.; Mouronval, G. Evaluation of the Petrophysical Properties of a Carbonate-rich Caprock for CO2 Geological Storage Purposes. In Proceedings of the 72nd European Association of Geoscientists and Engineers Conference and Exhibition 2010 A New Spring for Geoscience Barcelona, Spain 14-17 June 2010; Volume 2, pp. 802–814.
4. Espinoza, D.N.; Santamarina, J.C. Water-CO_2-mineral systems: Interfacial tension, contact angle, and diffusion—Implications to CO_2 geological storage. *Water Resour. Res.* **2010**, *46*. https://doi.org/10.1029/2009wr008634.
5. Broseta, D.; Tonnet, N.; Shah, V. Are rocks still water-wet in the presence of dense CO2 or H2S? *Geofluids* **2012**, *12*, 280–294. https://doi.org/10.1111/j.1468-8123.2012.00369.x.
6. Jung, J.-W.; Wan, J. Supercritical CO_2 and Ionic Strength Effects on Wettability of Silica Surfaces: Equilibrium Contact Angle Measurements. *Energy Fuels* **2012**, *26*, 6053–6059. https://doi.org/10.1021/ef300913t.
7. Farokhpoor, R.; Bjørkvik, B.J.; Lindeberg, E.; Torsæter, O. CO2 Wettability Behavior During CO2 Sequestration in Saline Aquifer -An Experimental Study on Minerals Representing Sandstone and Carbonate. *Energy Procedia* **2013**, *37*, 5339–5351. https://doi.org/10.1016/j.egypro.2013.06.452.
8. Seyyedi, M.; Sohrabi, M.; Farzaneh, A. Investigation of Rock Wettability Alteration by Carbonated Water through Contact Angle Measurements. *Energy Fuels* **2015**, *29*, 5544–5553. https://doi.org/10.1021/acs.energyfuels.5b01069.
9. Iglauer, S.; Mathew, M.; Bresme, F. Molecular dynamics computations of brine–CO2 interfacial tensions and brine–CO2–quartz contact angles and their effects on structural and residual trapping mechanisms in carbon geo-sequestration. *J. Colloid Interface Sci.* **2012**, *386*, 405–414. https://doi.org/10.1016/j.jcis.2012.06.052.
10. Tsuji, S.; Liang, Y.; Kunieda, M.; Takahashi, S.; Matsuoka, T. Molecular Dynamics Simulations of the CO2-Water-silica Interfacial Systems. *Energy Procedia* **2013**, *37*, 5435–5442. https://doi.org/10.1016/j.egypro.2013.06.462.
11. Chen, C.; Dong, B.; Zhang, N.; Li, W.; Song, Y. Pressure and Temperature Dependence of Contact Angles for CO_2/Water/Silica Systems Predicted by Molecular Dynamics Simulations. *Energy Fuels* **2016**, *30*, 5027–5034. https://doi.org/10.1021/acs.energyfuels.6b00171.
12. Yang, Y.; Nair, A.K.N.; Ruslan, M.F.A.C.; Sun, S. Interfacial properties of the alkane+water system in the presence of carbon dioxide and hydrophobic silica. *Fuel* **2021**, *310*, 122332. https://doi.org/10.1016/j.fuel.2021.122332.
13. Zhu, Z.; Li, M.; Lin, M.; Peng, B.; Sun, L.; Chen, L. Investigation on Variations in Wettability of Reservoir Rock Induced by CO_2-Brine-rock Interactions. In Proceedings of the SPE EUROPEC/EAGE Annual Conference and Exhibition, Vienna, Austria, 23–26 May 2011; Volume 5, pp. 4027–4038.
14. Yang, D.; Gu, Y. Interfacial Interactions of Crude Oil-Brine-CO_2 Systems under Reservoir Conditions. SPE Annual Technical Conference and Exhibition. In Proceedings of the SPE Annual Technical Conference and Exhibition, Houston, TX, USA, 26–29 September 2004.
15. McCaughan, J.; Iglauer, S.; Bresme, F. Molecular Dynamics Simulation of Water/CO2-quartz Interfacial Properties: Application to Subsurface Gas Injection. *Energy Procedia* **2013**, *37*, 5387–5402. https://doi.org/10.1016/j.egypro.2013.06.457.
16. Chen, C.; Chai, Z.; Shen, W.; Li, W.; Song, Y. Wettability of Supercritical CO_2–Brine–Mineral: The Effects of Ion Type and Salinity. *Energy Fuels* **2017**, *31*, 7317–7324. https://doi.org/10.1021/acs.energyfuels.7b00840.
17. Al-Mutairi, S.M.; Abu-Khamsin, S.A.; Okasha, T.M.; Aramco, S.; Hossain, M.E. An experimental investigation of wettability alteration during CO_2 immiscible flooding. *J. Pet. Sci. Eng.* **2014**, *120*, 73–77. https://doi.org/10.1016/j.petrol.2014.05.008.
18. Ali, M.; Arif, M.; Sahito, M.F.; Al-Anssari, S.; Keshavarz, A.; Barifcani, A.; Stalker, L.; Sarmadivaleh, M.; Iglauer, S. CO_2-wettability of sandstones exposed to traces of organic acids: Implications for CO_2 geo-storage. *Int. J. Greenh. Gas Control* **2019**, *83*, 61–68. https://doi.org/10.1016/B978-012370624-9/50005-0.
19. da Costa, A.A.; Costa, G.; Embiruçu, M.; Soares, J.B.; Trivedi, J.J.; Rocha, P.S.; Souza, A.; Jaeger, P. The Influence of Rock Composition and pH on Reservoir Wettability for Low-Salinity Water-CO_2 Enhanced Oil Recovery Applications in Brazilian Reservoirs. *SPE Reserv. Evaluation Eng.* **2020**, *24*, 45–65. https://doi.org/10.2118/195982-pa.
20. Ali, M.; Awan, F.U.R.; Ali, M.; Al-Yaseri, A.; Arif, M.; Sánchez-Román, M.; Keshavarz, A.; Iglauer, S. Effect of humic acid on CO_2-wettability in sandstone formation. *J. Colloid Interface Sci.* **2020**, *588*, 315–325. https://doi.org/10.1016/j.jcis.2020.12.058.

21. Ali, M.; Al-Yaseri, A.; Awan, F.U.R.; Arif, M.; Keshavarz, A.; Iglauer, S. Effect of water-soluble organic acids on wettability of sandstone formations using streaming zeta potential and NMR techniques: Implications for CO_2 geo-sequestration. *Fuel* **2022**, *329*. https://doi.org/10.1016/j.fuel.2022.125449.
22. Liu, S.; Yang, X.; Qin, Y. Molecular dynamics simulation of wetting behavior at CO_2/water/solid interfaces. *Chin. Sci. Bull.* **2010**, *55*, 2252–2257. https://doi.org/10.1007/s11434-010-3287-0.